J. Nat. Acad. Math. ISSN 0970-5228
Vol. 34 (2020), pp.1-14

MHD Flow and Heat Transfer in a Channel filled with Variable Permeability Porous Layers

By

Manju Agarwal[1], Deepak Kumar[2] and V. S. Verma[3]

Abstract

The present paper addresses magnetohydrodynamic (MHD) flow and heat transfer of two immiscible, incompressible, and conductive fluids in a channel filled with variable permeability porous layers. The flow in clear fluid region is assumed to be governed by Navier-Stokes equation, whereas the dynamics of porous region is determined by Darcy's law. In the study, matching conditions are used at the interface. The governing equations are evaluated numerically and the results are depicted through graphs.

Key words : Conducting fluid, Porous media, Darcy's law, Runge-Kutta method.

1. Introduction

In the past few decades, the study of multiphase flow and heat transfer in the porous channels is increasingly studied. This research area has large scale potential in engineering and geophysical applications. Some major applications are in the petroleum industry for studying the flow of hydrocarbons in reservoir rocks; in agricultural engineering for studying surface and underground water flows; in geotechnical engineering for studying underground waste disposal; and in nuclear engineering for designing pebble bed reactors. Other applications include sewage, porous bearings, solid matrix heat exchangers, and bioconvection in porous media. Blood flow has been considered as two fluid flow by many researchers[14][15][16].

M. Hribersek[1] investigated the influence of porous domains with relatively high values of permeability on the flow inside a narrow channel. Tien-Chien Jen and T.Z. Yan[2] analyzed developing fluid flow and heat transfer in a channel partially filled with porous medium and developed a three dimensional model. They found that as the porous ratio increases, the flow in the fluid layer also increases. Flow through composite porous layers of variable permeability is investigated by M. S. Abu Zayton[3]. They presented solutions of flow in terms of Airy's and the

Received : March 17, 2020; Accepted : October 29, 2020

Nield-Koznetsov function. M. Chandesni and D. Jamet[4] discussed about the velocity boundary conditions that must be imposed at an interface between a porous medium and a free fluid. R.A. Ford and M.H. Hamdan[5] analyzed a fluid flow through composite porous layers by using matching conditions at the interface. They Concluded that for low permability, an increase in permeability results in an increase in both the velocity and shear stress at the interface. A plain Poiseuille flow through variable permeability porous layers is analyzed by M.H. Hamdan and M. T. Kamel[6]. They found a new dimensionless number, H_a, and said that the number might be useful in analysis of general variable permeability media.

B. Alazami and K. Vafai[7] investigated fluid flow and heat transfer in interfacial conditions between a porous medium and a fluid layer and provided a set of correlations for interchanging the interfacial velocity, the interfacial temperature and the average Nusselt number among different models. M. Sahraoui and M. Kaviang[8] examined hydrodynamic boundary conditions at the interface between a porous and a plain medium. Effects of porosity on MHD two fluid flow in an inclined channel are studied by Jafar Hasnain et. al.[9]. They found that temperature distribution decreases with the increase in the magnetic parameter throughout the channel. M. S. Abu Zaytoon et.al.[10] investigated a flow through a variable permeability Brinkman porous layers with quadratic permeability funtion by using matching conditions at the interface. They considered the flow in a channel having two layers out of which, one is Darcy layer and the other Brinkman layer. They assumed that the permeability in the Darcy layer to be an increasing linear function, and in Brinkman layer, a quadratic permeability function. S. O. Alharbi[11] studied the problem of laminar flow through a porous medium by introducing permeability variations in the governing flow equations. Bal Govind Srivastava and Satya Deo[12] discussed the effects of magnetic field on the fluid flow in a channel filled with porous medium of variable permeability. They found that as the value of Hartmann number increases, the velocity decreases. Variable permeability effects in binary mixtures saturating a porous layer is studied by Z. Alloui et.al.[13]. They assumed the permeability of the medium to vary exponentially with the depth of the layer.

2. Mathematical Formulation

Consider the flow of two electrically conducting immiscible Newtonian fluids in a channel of height h_2, partially filled with porous layers of different permeabilities up to height h_1. The flow geometry is described if Fig. 1. Origin is at the lower wall of the channel and X and Y are horizontal and vertical coordinates

respectively. The Region I $(0 \leq y \leq h_1)$ is occupied by an electrically conducting fluid of density ρ_1, viscosity μ_1, electric conductivity σ_1 and thermal conductivity k_1. The Region II $(h_1 \leq y \leq h_2)$ is filled with an electrically conducting fluid of density $\rho_2 (< \rho_1)$, viscosity μ_2, electric conductivity σ_2 and thermal conductivity k_2. The lower and upper plates are held at different constant temperatures T_{w_1} and T_{w_2}, respectively with $T_{w_2} > T_{w_1}$.

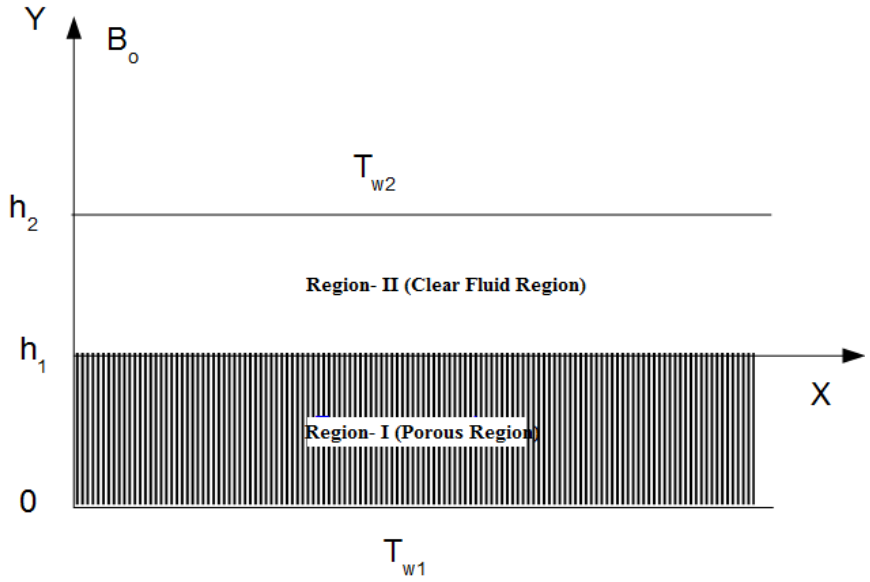

FIGURE 1. Schematic diagram of Two Fluid Flow

Let us assume that the permeability of the porous region $0 \leq y \leq h_1$, is a quadratic, parabolic function of y, with a value K_o at $y = h_1$ and $K_o\epsilon$ at the lower wall of the channel. Now, let

$$K(y) = ay^2 + by + c, \tag{2.1}$$

$$K(0) = K_o\epsilon, \; K(h_1) = K_o. \tag{2.2}$$

where ϵ is a non-dimensional parameter lying in the closed interval $[0, 1]$ and a is arbitrary dimensionless constant.

Using conditions (2.2) in equation (2.1), we get

$$K(y) = a(y^2 - h_1 y) + \frac{K_o}{h_1} y + K_o\epsilon \left(1 - \frac{y}{h_1}\right). \tag{2.3}$$

Using the Lagrange's necessary and sufficient conditions for maxima and minima, we find that, if $a < 0$, maximum value of $K(y)$ occurs at $y = \frac{h_1}{2}(1 - \frac{K_o(1-\epsilon)}{ah_1^2})$. Further, if $K_o(1-\epsilon) + ah_1^2 = 0$, we get maximum value at $y = h_1$ and if $0 < K_o(1-\epsilon) + ah_1^2 < ah_1^2$, then maximum value occurs in the region $\frac{h_1}{2} < y < h_1$.

Assuming the flow in both regions to be one dimensional, laminar and driven only by a constant pressure gradient $\frac{dp}{dx}$, applied at the mouth of the channel, velocity and temperature distributions are given by

2.1. Velocity distributions

The governing equation in Region-I is

$$-\frac{dp}{dx} + \mu_1 \frac{d^2u_1}{dy^2} - \frac{\mu_1}{K(y)}u_1 - \sigma_1 B_0^2 u_1 = 0. \tag{2.4}$$

The governing equation in Region-II is

$$-\frac{dp}{dx} + \mu_2 \frac{d^2u_2}{dy^2} - \sigma_2 B_0^2 u_2 = 0. \tag{2.5}$$

Let the walls of the channel be impermeable and fixed, so that no slip condition can be applied at the lower and upper permeable walls i.e.

$$\begin{aligned} u_1(y) &= 0 \quad \text{at } y = 0, \\ u_2(y) &= 0 \quad \text{at } y = h_2. \end{aligned} \tag{2.6}$$

Also, fluids in both regions are immiscible so velocity and shear stress are continuous at the interface i.e.

$$\left.\begin{aligned} u_1(y) = u_2(y) \\ \mu_1 \tfrac{du_1}{dy} = \mu_2 \tfrac{du_2}{dy} \end{aligned}\right\} \quad \text{at } y = h_1, \tag{2.7}$$

where u_1 and u_2 are the flow velocities in Region-I and Region- II, respectively and B_o is the magnetic field applied in the direction normal to the flow.

2.2. Temperature distribution

The governing equation in Region-I is

$$k_1 \frac{d^2T_1}{dy^2} + \mu_1 \left(\frac{du_1}{dy}\right)^2 + \frac{\mu_1}{K(y)}u_1^2 + \sigma_1 B_o^2 u_1^2 = 0. \tag{2.8}$$

The governing equation in Region-II is

$$k_2\frac{d^2T_2}{dy^2}+\mu_2\left(\frac{du_2}{dy}\right)^2+\sigma_2B_o^2u_2^2=0. \tag{2.9}$$

The lower and upper walls of the channel are at constant temperatures, so we have

$$\begin{aligned} T_1(y) &= T_{w_1} \quad \text{at } y=0, \\ T_2(y) &= T_{w_2} \quad \text{at } y=h_2. \end{aligned} \tag{2.10}$$

Also, temperature and heat fluxes are continuous at the interface i.e.

$$\left.\begin{array}{c} T_1(y)=T_2(y) \\ k_1\frac{dT_1}{dy}=k_2\frac{dT_2}{dy} \end{array}\right\} \quad \text{at } y=h_1, \tag{2.11}$$

where T_1 and T_2 are the temperatures in Region-I and Region- II, respectively.

3. Non-dimensionalization of flow quantities

Introducing the following non-dimensional quantities

$$\left.\begin{array}{c} x^*=\frac{x}{h_2}, y^*=\frac{y}{h_2}, u_i^*=\frac{u_i}{u}, p^*=\frac{p}{\rho_1u^2} \\ K^*(y)=\frac{K(y)}{K_o}, \theta_i^*=\frac{T_i-T_{w_1}}{T_{w_2}-T_{w_1}} \end{array}\right\}, i=1,2, \tag{3.1}$$

and dropping asterisks, velocity distribution and temperature distribution in non-dimensional form are given as

3.1. Velocity distribution

Governing equations (2.4) and (2.5), respectively, become:

$$\frac{d^2u_1}{dy^2}-\frac{1}{aD_aK(y)}u_1-M^2u_1=R_1\frac{dp}{dx} \tag{3.2}$$

$$\frac{d^2u_2}{dy^2}-M^2\frac{\sigma'}{\mu'}u_2=\frac{R_2}{\rho'}\frac{dp}{dx}. \tag{3.3}$$

The boundary and interface conditions become:

$$\begin{aligned} u_1(y) &= 0 \quad \text{at } y = 0 \\ u_2(y) &= 0 \quad \text{at } y = 1 \end{aligned} \tag{3.4}$$

$$\left.\begin{aligned} u_1(y) = u_2(y) \\ \tfrac{du_1}{dy} = \mu' \tfrac{du_2}{dy} \end{aligned}\right\} \quad \text{at } y = h, \tag{3.5}$$

where $\sigma' = \frac{\sigma_2}{\sigma_1}$, $\mu' = \frac{\mu_2}{\mu_1}$ and $\rho' = \frac{\rho_2}{\rho_1}$ are electric conductivity ratio, viscosity ratio, and density ratio, respectively. $R_1 = \frac{\rho_1 u h}{\mu_1}$, $R_2 = \frac{\rho_2 u h}{\mu_2}$ are non-dimensional parameters, known as Reynold's numbers. $M = B_o h \sqrt{\frac{\sigma_1}{\mu_1}}$ is the Hartmann number.

3.2. Temperature distribution

Governing equations (2.8) and (2.9), respectively, becomes:

$$\frac{d^2\theta_1}{dy^2} + E_c P_r \left(\frac{du_1}{dy}\right)^2 + \frac{1}{aD_a K(y)} E_c P_r u_1^2 + M^2 E_c P_r u_1^2 = 0 \tag{3.6}$$

$$k' \frac{d^2\theta_2}{dy^2} + \mu' E_c P_r \left(\frac{du_2}{dy}\right)^2 + \sigma' M^2 E_c P_r u_2^2 = 0. \tag{3.7}$$

The boundary and interface conditions become:

$$\begin{aligned} T_1(y) &= 0 \quad \text{at } y = 0 \\ T_2(y) &= 1 \quad \text{at } y = 1 \end{aligned} \tag{3.8}$$

$$\left.\begin{aligned} T_1(y) = T_2(y) \\ \tfrac{dT_1}{dy} = k' \tfrac{dT_2}{dy} \end{aligned}\right\} \quad \text{at } y = h, \tag{3.9}$$

where $K(y) = \frac{1}{D_a}(y^2 - hy) + \frac{y}{h} + \epsilon(1 - \frac{y}{h})$ is the permeability of the porous region in non-dimensional form. $D_a = \frac{K_o}{a h_2^2}$ is the non-dimensional parameter. Where $E_c = \frac{u^2}{C_p(T_{w_2} - T_{w_1})}$, $P_r = \frac{\mu_1 C_p}{k_1}$ and $k' = \frac{k_2}{k_1}$ are Eckert number, Prandtl number and viscosity ratio, respectively.

The number D_a is a dimensionless number, depends on the channel height h_2, permeability of the upper most layer of the porous region K_o and a constant a. For maximum value of $K(y)$, the constant a must be negative therefore D_a is always negative. Also the maximum value of $K(y)$ occurs at $y = \frac{h}{2}(1 - \frac{D_a(1-\varepsilon)}{h^2})$,

which shows that the number D_a determines position of maximum value (Fig.2). When $\epsilon \neq 1$, if $D_a = -\frac{h^2}{(1-\epsilon)}$ then maximum value occurs at $y = h$ (i.e. at the top of the porous region) and for $-\frac{h^2}{(1-\epsilon)} < D_a < 0$, the maximum value occurs in the region $\frac{h}{2} < y < h$. Also as $D_a \to 0$, maxima shifted towards the mid of the porous region. When $\epsilon = 1$, we get maximum permeability in the mid ($y = \frac{h_1}{2}$) of the porous region.

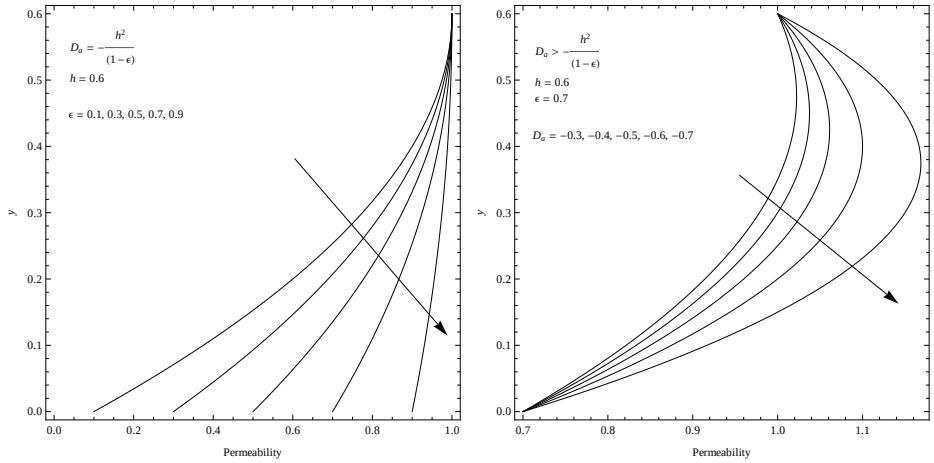

(a) (b)

FIGURE 2. Permeability variation in Region I

4. Numerical results and discussions

The solution of the problem in terms of velocity and temperature distributions is obtained numerically by employing a shooting method with Runge-Kutta method of order four having classical coefficients for various values of the parameters. The results are depicted graphically in Figs. 3–8. In the numerical evaluation, we take $R_2 = \frac{\rho'}{\mu'} R_1$, $D_a = -1.25$ (For the case $D_a = -\frac{h^2}{(1-\epsilon)}$), and $D_a = -0.50$ (For the case $D_a > -\frac{h^2}{(1-\epsilon)}$).

Figure 3(a) depict the variation in flow velocity with respect to non-dimensional constant a. The velocity decreases with an increase in a.This is due to the fact that as a increases, D_a decreases, which in turn decreases the permeability of the porous medium. Velocity profiles with respect to Hartmann number M are presented in Fig. $3(b)$. The flow velocity decreased with an increase in M. The effect of magnetic field is more catchy at the point of peak value that is the peak value substantially decreased with increase in magnetic field. The decrement in

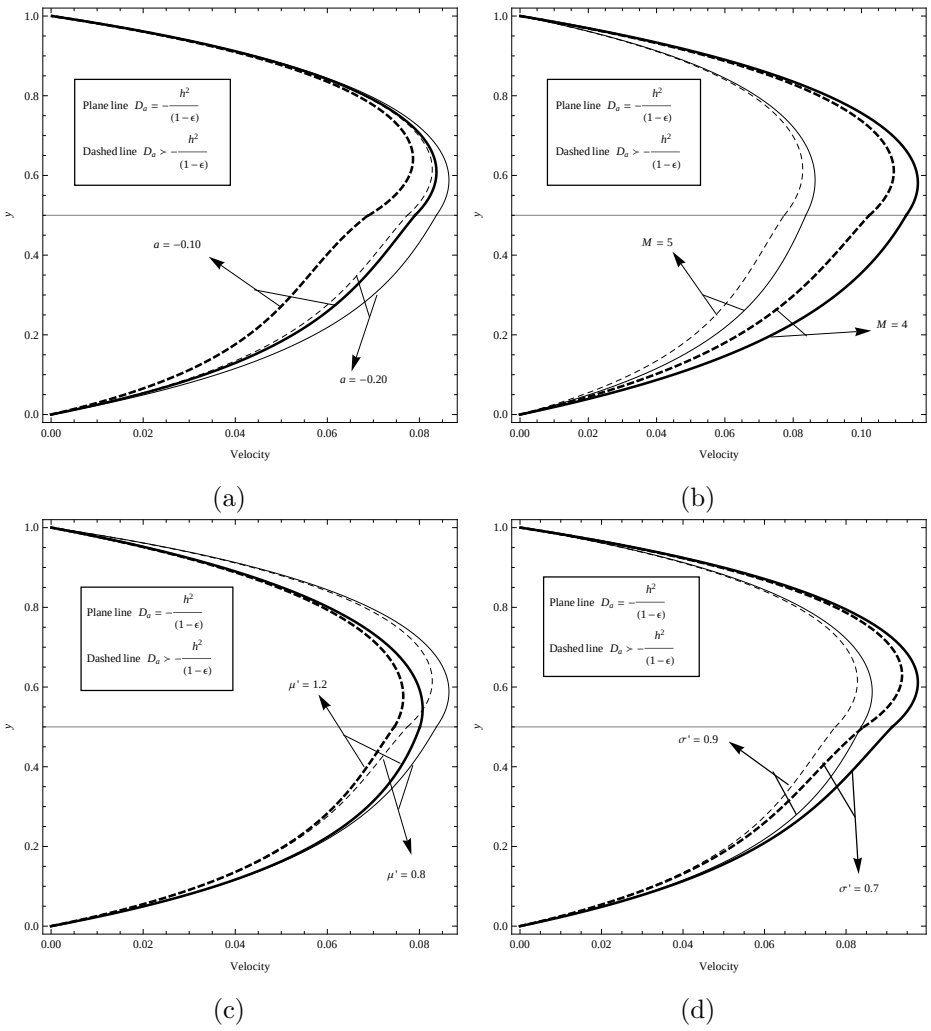

FIGURE 3. Velocity profiles for different flow parameters at $M = 5$, $\sigma' = 0.9$, $\mu' = 00.8$, $\rho' = 0.9$, $k' = 0.9$, $P = -5$, $E_c = 1$, $P_r = 1$, $R_1 = 0.5$, $h = 0.5$, $\epsilon = 0.8$, $a = -0.20$ except where they are variable.

velocity is due to the presence of magnetic field in normal direction to the flow, which introduces Lorentz force acting against the flow. The velocity in both the regions decreased with an increased in μ' (Fig.3(c)) because as μ' increases, fluids become thicker. Further as μ' increased, peak velocity shifts towards the mid of the channel. Variation in velocity profiles with respect to σ' are almost similar as for μ' (Fig. 3(d)).

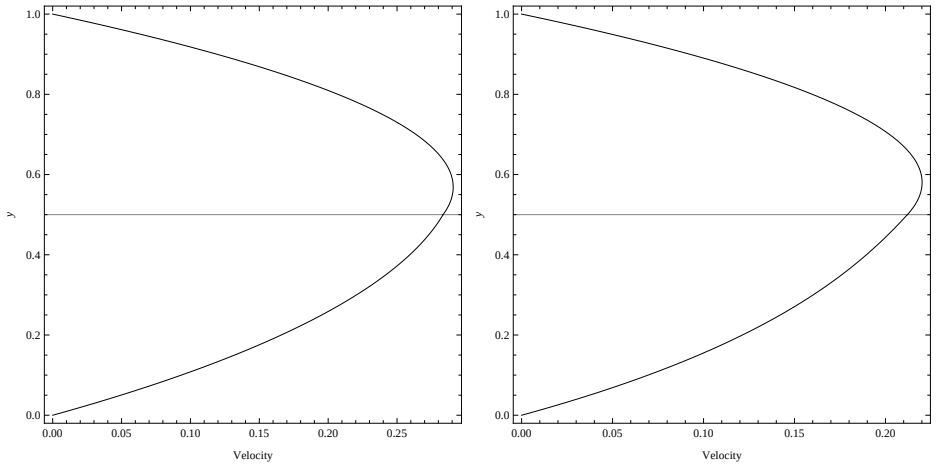

(a) Velocity profile for different fluids at $M = 0$.

(b) Velocity profile for same fluids at $M = 0$.

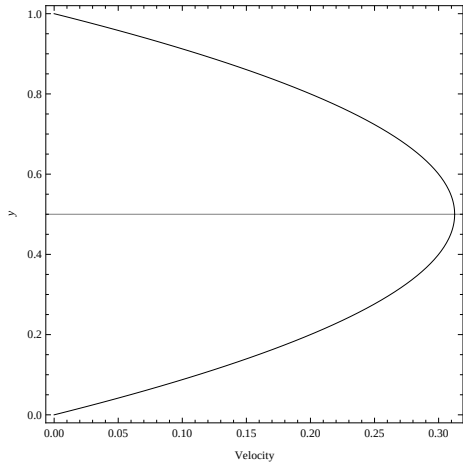

(c) Velocity profile for same fluids at $M = 0$ and $K(y) \to \infty$.

FIGURE 4. Some particular cases of velocity profiles.

In absence of the magnetic field, velocity profile is depicted in Fig. $4(a)$. Fig. $4(b)$ represents the velocity profile, when $M = 0$ and fluids in both the regions are same. In addition to above, when permeability of the region I tends to infinity, velocity profile is shown in Fig. $4(c)$. In this case, velocity profiles resembles the Hagen-Poiseuille flow.

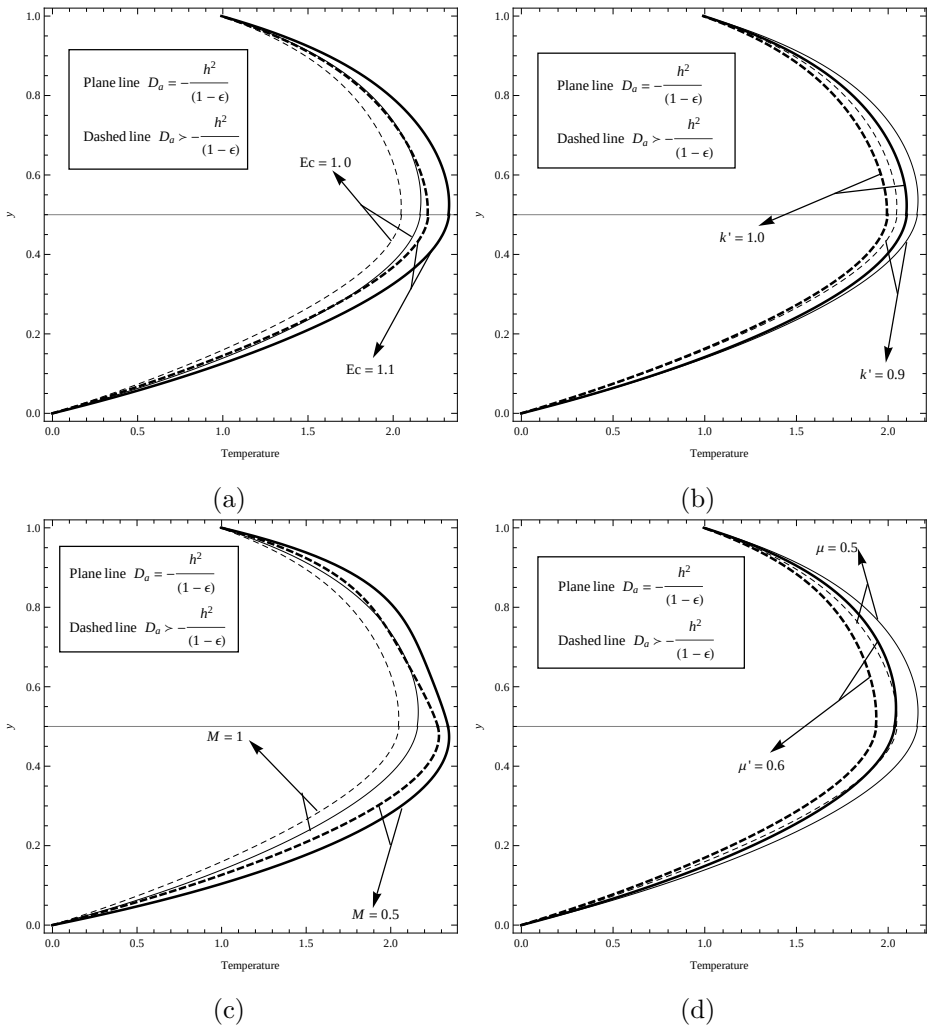

FIGURE 5. Temperature profiles for different flow parameters at $M = 5$, $\sigma' = 0.9$, $\mu' = 00.8$, $\rho' = 0.9$, $k' = 0.9$, $P = -5$, $E_c = 1$, $P_r = 1$, $R_1 = 0.5$, $h = 0.5$, $\epsilon = 0.8$, $a = -0.20$ except where they are variable.

Figs. 5–7 depict the variations in temperature with respect to Eckert number E_c, thermal conductivity ratio k', Hartmann number M, viscosity ratio μ', Prandtl number P_r and electric conductivity ratio σ'. From Fig. $5(a)$, it is observed that as E_c increases, the temperature profile also increases. Increment in E_c results in increment in fluid frictional effects, which enhance the temperature of the fluids. The temperature decreases with an increase in k' (Fig.5(b)), M

(Fig.5(c)), and μ' (Fig. 5(d)). From Fig. 6(a), it can be observed that as Pr increases, the temperature profile also increases. Increment in P_r results in increment in viscous diffusion in the presence of viscous dissipation, which enhances internal heat generation. The temperature decreases with an increase in σ' (Fig. 6(b)). Fig. 7(a) depicts the variation in temperature profile when the fluids in the both regions are considered to be same. In addition when $M = 0$, temperature profile is presented in Fig. 7(b). Further, when porosity of the porous medium is tending to infinity, the temperature profile is depicted in Fig. 7(c).

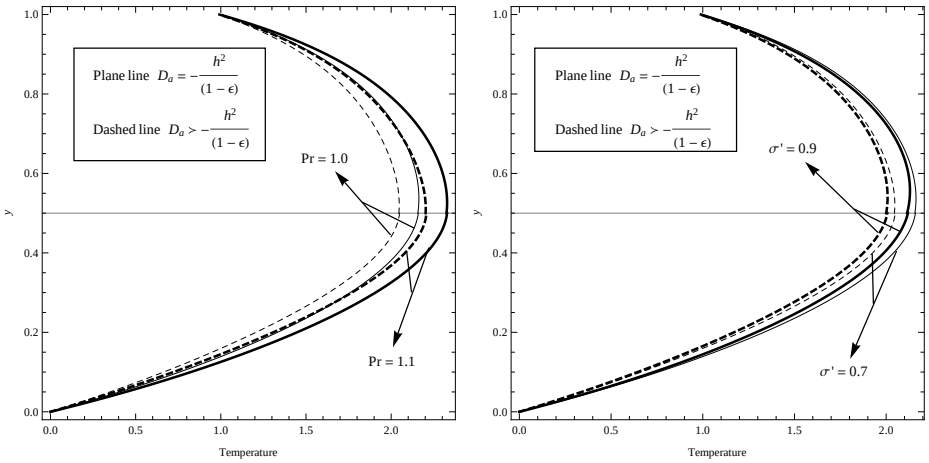

(a) (b)

FIGURE 6. Temperature profiles for different flow parameters at $M = 5$, $\sigma' = 0.9$, $\mu' = 00.8$, $\rho' = 0.9$, $k' = 0.9$, $P = -5$, $E_c = 1$, $P_r = 1$, $R_1 = 0.5$, $h = 0.5$, $\epsilon = 0.8$, $a = -0.20$ except where they are variable.

5. Conclusion

We discussed MHD fluid flow and heat transfer of two immiscible, incompressible, and conducting fluids in a channel filled with variable permeability porous layers. The solution of the problem was obtained numerically by employing a shooting method with Runge-Kutta method of order 4 having classical coefficients. The effects of flow parameters on the flow velocity and temperature variations are depicted through graphs. The following conclusions can be drawn from the entire analysis:

- If $D_a = -\frac{h^2}{1-\epsilon}$ then maximum value of the permeability occurs at top of the channel and for $-\frac{h^2}{1-\epsilon} < D_a < 0$, the maximum value occurs at some middle point in the porous region.

- The velocity profile is decreasing function of dimensionless constant a and Hartmann number.
- As viscosity ratio and electric conductivity ratio decrease, the velocity profile increases.
- The temperature profile is an increasing function of Eckert number and Prandtl number, whereas it behaves like decreasing function of thermal and electric conductivity ratios.

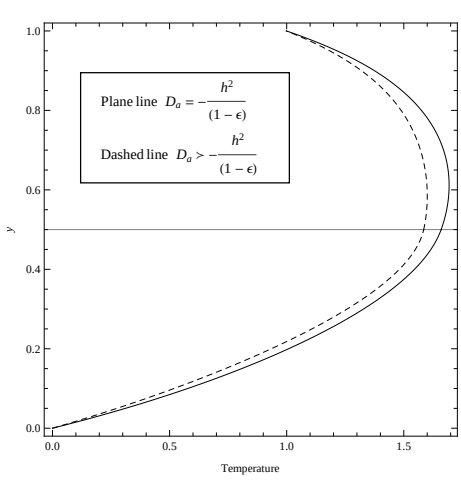

(a) Temperature profile for same fluids.

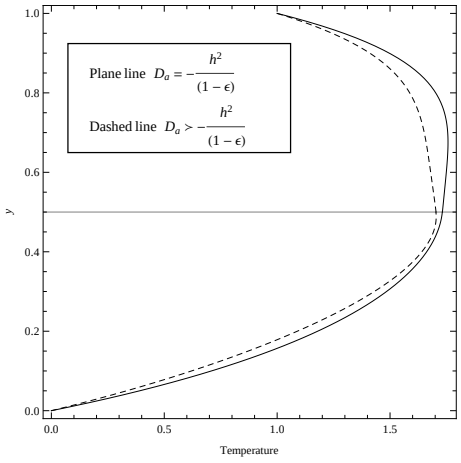

(b) Temperature profile for same fluids at $M = 0$

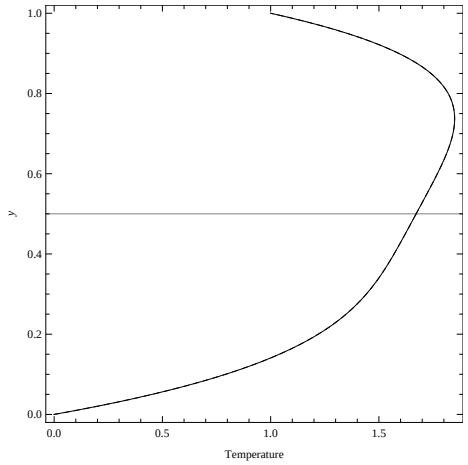

(c) Temperature profile for same fluids at $M = 0$ and $K(y) \to \infty$.

FIGURE 7. Some particular cases of temperature profiles.

[1]Department of Mathematics and Astronomy
University of Lucknow, Lucknow-226007, India.
E-mail : manjuak@yahoo.com
[2]Department of Mathematics
T. P. Varma College, Narkatiaganj,
West Champaran-845455, India.
E-mail : deepakmaths@yahoo.com
[3]Department of Mathematics and Statistics
Deen Dayal Upadhyaya Gorakhpur University
Gorakhpur-273009, India.
E-mail : drvsverma01@gmail.com

References

[1] **Hribersek, M. et.al.:** Fluid flow in a channel partially filled with porous material, Advances in fluid mechanics IV, 36 (2002), 465–472.

[2] **Tien-Chien Jen and Yan, T.Z.:** Developing fluid flow and heat transfer in a channel partially filled with porous medium, International Journal of Heat and Mass Transfer, 48 (2005), 3995–4009.

[3] **Abu Zaytoon, M. S.:** Flow through a Variable Permeability Brinkman Porous Core, Journal of Applied Mathematics and Physics, 4 (4) (2016), 766–778.

[4] **Chandesris, M. and Jamet, D.:** Boundary conditions at a planar fluid–porous interface for a Poiseuille flow, International Journal of Heat and Mass Transfer 49 (2006), 2137–2150.

[5] **Ford, R. A. and Hamdan, M. H.:** Coupled parallel flow through composite porous layers, Applied Mathematics and Computation 97 (1998), 261–271.

[6] **Hamdan, M. H. and Kamel, M. T.:** Flow through Variable Permeability Porous Layers, Adv. Theor. Appl. Mech., 4 (3) (2011), 135–145.

[7] **Alazmi, B. and Vafai, K.:** Analysis of fluid flow and heat transfer interfacial conditions between a porous medium and a fluid layer, International Journal of Heat and Mass Transfer 44 (2001) 1735–1749.

[8] **Sahraoui, M. and Kaviany, M.:** Slip and no-slip velocity boundary conditions at interface of porous, plain media, InI. J. Heat Mass Transfer, 35 (4) (1992), 927–94.

[9] **Hasnain, Jafar et.al.:** Effects of Porosity and Mixed Convection on MHD Two Phase Fluid Flow in an Inclined Channel, PLoS ONE 10 (3) (2015), 1–16.

[10] **Abu Zaytoon, M. S. et.al.:** Flow through Variable Permeability Composite Porous Layers, Gen. Math. Notes, 33 (1), (2016), 26–39.

[11] **Alharbi, S. O. et.al.:** Permeability Variations in Laminar Flow through a Porous Medium Behind a Two-dimensional Grid, IOSR Journal of Engineering, 6 (5) (2016), 42–55.

[12] **Srivastava, Bal Govind and Satya Deo:** Effect of magnetic field on the viscous fluid flow in a channel filled with porous medium of variable permeability, Applied Math ematics and Computation, 219 (2013), 8959–8964.

[13] **Alloui, Z. et.al.:** Variable permeability effect on convection in binary mixtures saturating a porous layer, Heat and Mass Transfer, 45 (8) (2009), 1117–1127.

[14] **Chaturani, P. and Samy, R. P.:** A study of non-Newtonian aspects of blood flow through stenosed arteries and its applications in arterial diseases, Biorheology, 22 (6) (1985), 521–531.

[15] **Sharan, M. and Popel, A. S.:** A two-phase model for flow of blood in narrow tubes with increased effective viscosity near the wall, Biorheology, 38 (5–6) (2001), 415–428.

[16] **Garcia, A. E. and Riahi, D. N.:** Two phase blood flow and heat transfer in an inclined stenosed artery with or without a catheter, Int. J. Fluid Mech. Res., 41 (1) (2014), 16–30